AIP | The Journal of Chemical Physics

Diffusiophoresis of a nonuniformly charged sphere in an electrolyte solution

Xuan-Cuong Luu, Jyh-Ping Hsu, and Shiojenn Tseng

Citation: The Journal of Chemical Physics **134**, 064708 (2011); doi: 10.1063/1.3548654
View online: http://dx.doi.org/10.1063/1.3548654
View Table of Contents: http://scitation.aip.org/content/aip/journal/jcp/134/6?ver=pdfcov
Published by the AIP Publishing

Diffusiophoresis of a nonuniformly charged sphere in an electrolyte solution

Xuan-Cuong Luu,[1,a)] Jyh-Ping Hsu,[1,b)] and Shiojenn Tseng[2]
[1]*Department of Chemical Engineering, National Taiwan University, Taipei, Taiwan 10617*
[2]*Department of Mathematics, Tamkang University, Tamsui, Taipei, Taiwan 25137*

(Received 23 August 2010; accepted 23 December 2010; published online 10 February 2011)

The diffusiophoresis of a rigid, nonuniformly charged spherical particle in an electrolyte solution is analyzed theoretically focusing on the influences of the thickness of double layer, the surface charge distribution, the effect of electrophoresis, and the effect of double-layer polarization. We show that the nonuniform charge distribution on the particle surface yields complicated effect of double-layer polarization, leading to interesting diffusiophoretic behaviors. For example, if the sign of the middle part of the particle is different from that of its left- and right-hand parts, then depending upon the charge density and the fraction of the middle part, the particle can move either to the high-concentration side or to the low-concentration side. Both the diffusiophoretic velocity and its direction can be manipulated by the distribution of the surface charge density. In particular, if the electrophoresis effect is significant, then those properties are governed by the averaged surface charge density of the particle. A dipolelike particle, where its left- (right-) hand half is negatively (positively) charged, always migrates toward the low-concentration (left-hand) side, that is, it has a negative diffusiophoretic velocity. In addition, that diffusiophoretic velocity has a negative local minimum as the thickness of double layer varies. © *2011 American Institute of Physics*. [doi:10.1063/1.3548654]

I. INTRODUCTION

Diffusiophoresis, the spontaneous movement of a colloidal particle subjected to an applied concentration gradient, was first investigated theoretically by Dukhin and Deryagin[1] through considering an isolated, rigid, charged spherical particle having a thin double layer in an infinite electrolyte solution imposed with a uniform concentration gradient, followed by several theoretical analyses[2–6] and experiment studies.[7–12] This phenomenon has many applications in practice, including, for instance, scavenging of radioactive particles in atmosphere,[13] ionic deposition and film coating process,[8,12,14,15] and separation of micron-sized particles from air.[16] Diffusiophoresis can be driven by van der Walls force[2,10] and dipole force in nonelectrolyte solutions, and by electrostatic force in electrolyte media.[3,5,6,11] For the case of a uniformly charged particle, the observed diffusiophoretic behaviors are usually explained by the polarization of its double layer and the presence of a background electric field arising from the difference in ionic diffusivities.[4,5,17] In a study of the diffusiophoresis of an isolated, uniformly charged, rigid sphere in an infinite electrolyte solution, Prieve and Roman[5] showed that the driving force exerting on the sphere comprises a chemiphoresis component and an electrophoresis component. The former comes from the nonuniform accumulation of ionic species inside the double layer and the latter from the difference in ionic diffusivities. Hsu *et al.*[17] suggested that two types of double-layer polarization (DLP) might present: type I DLP, which drives the particle toward the high-concentration side, arises from the nonuniform distribution of counterions inside the double layer, and type II DLP, which drives the particle toward the low-concentration side, comes from the nonuniform distribution of coions immediately outside the double layer. In general, type I DLP is more significant than type II DLP, and the latter is enhanced when the surface potential is high and the double layer is thin. Recently, Lee *et al.*[18] modeled the diffusiophoresis of a uniformly charged sphere along the axis of a cylindrical pore, and that of a uniformly charged elongated cylindrical particle was considered by Joo *et al.*,[19] Lee *et al.*[20] and Yalcin *et al.*[21] analyzed the electrodiffusiophoresis of a uniformly charged sphere along the axis of a cylindrical pore.

Colloid particles having a nonuniformly charged surface are not uncommon in reality. Examples include, for instance, rods having different chemical structures at their two ends,[22] spheres with asymmetrically distributed enzymatic sites,[23] polymer chains having alternating positive and negative charges,[24] rutile hematite system,[25] and kaolinite.[26] If the surface of a particle is nonuniformly charged, then the associated double layer may become asymmetric. This induces an ionic concentration gradient and an internal electric field inside the double layer, which influences the concentration, the electric field, and the flow fields near the particle and, therefore, its diffusiophoretic behavior. Previous efforts made on the analyses of electrokinetic phenomena and diffusiophoresis are based mainly on homogeneously charged particles. Considering the applications in practice, extending this type of particle to a more general case of nonuniformly charged conditions is highly desirable.

[a)]Tel.: 886–2-23637448. FAX: 886–2-236223040.
[b)]Author to whom correspondence should be addressed. Electronic mail: jphsu@ntu.edu.tw.

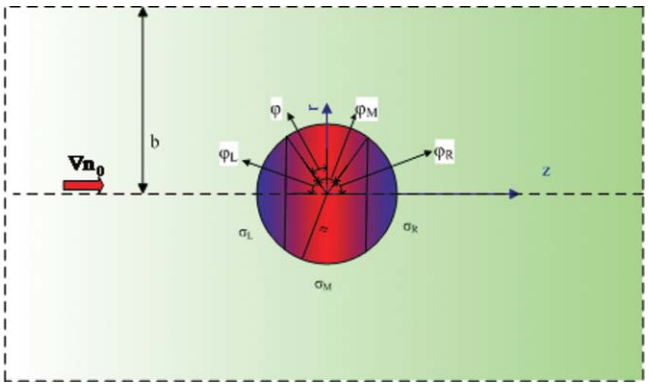

FIG. 1. Diffusiophoresis of a nonuniformly charged spherical particle of radius a as a response to an applied uniform concentration gradient ∇n_0. For convenience, a cylindrical computational domain of radius b ($b \gg a$) is defined, and the particle moves along the axis of that domain. The cylindrical coordinates r, θ, z with the origin at the center of the particle are adopted. σ_L, σ_M, and σ_R are the surface charge density on the left-hand, the middle, and the right-hand parts of the particle, respectively, defined by the azimuth angles ϕ_R, ϕ_M, and ϕ_L, respectively.

This study is aimed to investigate the effect of the nonuniformly charged conditions on the surface of a particle on its diffusiophoretic behavior. For illustration, we consider the case where a particle is divided into several parts, each can be charged differently with the other parts. Similar model was also considered by Qian *et al.*[27] and Qian and Joo[28] in electrophoresis problems. The diffusiophoresis behaviors of the particle under various conditions are discussed in detail. In particular, the influences of the charged conditions on the particle, the thickness of double layer, and the diffusivities of ionic species on the diffusiophoretic mobility of the particle are examined.

II. THEORY

Referring to Fig. 1, we consider the diffusiophoresis of the nonuniformly charged spherical particle of radius a as a response to an applied uniform concentration gradient ∇n_0. For convenience, a cylindrical computational domain of radius b ($b \gg a$) is defined, and the particle moves along the axis of that domain, which is filled an aqueous, incompressible Newtonian fluid containing $z_1 : z_2$ electrolytes with z_1 and z_2 being the valence of cations and that of anions, respectively. The cylindrical coordinates r, θ, z with the origin at the center of the particle are adopted. The particle is divided into the left-hand, the middle, and the right-hand parts, with surface charge densities, σ_L, σ_M, and σ_R, respectively, and the surface charge density of the particle σ_P is described by

$$\sigma_P = \begin{cases} \sigma_R, & 0 < \varphi_R < 90 - \varphi \\ \sigma_M, & 90 - \varphi < \varphi_M < 90 + \varphi \\ \sigma_L, & 90 + \varphi < \varphi_L < 180 \end{cases}, \tag{1}$$

where φ_L, φ_M, and φ_R are the azimuth angles specifying the left-hand side (LHS), the middle, and the right-hand parts of the particle, respectively. The charged conditions on the particle surface can be adjusted through varying the azimuth angle φ and the charge densities σ_R, σ_M, and σ_L. The net amount of ions inside the double layer of the particle correlates with the averaged charge density on the particle surface, $\overline{\sigma}$, defined by

$$\overline{\sigma} = \frac{\sigma_R S_R + \sigma_M S_M + \sigma_L S_L}{S_R + S_M + S_L}, \tag{2}$$

where S_R, S_M, and S_L are the surface areas of the right-, the middle, and the left-hand parts of the particle, respectively. Due to the θ-symmetric nature of the present problem, the sphere does not rotate, and only the (r,z) domain needs be considered.

The governing equations of the present problem include the following:

$$\nabla^2 \phi = -\frac{\rho}{\varepsilon} = -\sum_{j=1}^{2} \frac{z_j e n_j}{\varepsilon}, \tag{3}$$

$$\nabla \cdot \left[-D_j \left(\nabla n_j + \frac{z_j e}{k_B T} n_j \nabla \phi \right) + n_j \mathbf{v} \right] = 0, \tag{4}$$

$$-\nabla p + \mu \nabla^2 \mathbf{v} - \rho \nabla \phi = 0, \tag{5}$$

$$\nabla \cdot \mathbf{v} = 0. \tag{6}$$

These expressions are the Poisson equation describing the electric potential ϕ, the conservation of ionic species based on Nest–Plank equation, and the Navier–Stoke equation and the continuity equations describing the liquid velocity $\mathbf{v}$, respectively. Here, ∇, ∇^2 are the gradient operator and the Laplace operator, respectively; n_j, z_j, D_j, $j = 1,2$, are the number concentration, the valence, and the diffusivity of ionic species j, respectively; ε,μ are the permittivity and the viscosity of the liquid phase, respectively; ρ and p are the space charge density and the pressure, respectively; e, k_B, and T are the elementary charge, the Boltzmann constant, and the absolute temperature, respectively.

Suppose that the magnitude of the applied concentration gradient, $|\nabla n_0|$, is much smaller than (n_{0e}/a). In this case, each dependent variable can be expressed as the sum of an equilibrium component representing its value in the absence of ∇n_0 and a perturbed component arising from the application of ∇n_0.[27] That is, $\phi = \phi_e + \delta\phi$, $p = p_e + \delta p$, and $\mathbf{v} = \mathbf{v}_e + \delta\mathbf{v}$, where the subscript e and the prefix δ denote the equilibrium component and the perturbed component, respectively. Note that because the particle is stagnant at equilibrium, $\mathbf{v} = \mathbf{0}$, and therefore, $\mathbf{v} = \delta\mathbf{v}$. In addition, the expression below is assumed to take account of the possible polarization of the double layer surrounding the particle:[17,26,28]

$$n_j = n_{j0e} \exp\left[-\frac{z_j e}{k_B T} (\phi_e + \delta\phi + g_j) \right], \; j = 1, 2, \tag{7}$$

where n_{j0e} is the bulk concentration of ionic species j at equilibrium, and g_j is a hypothetical potential describing the deformation of the double layer. Then, it can be shown that Eqs. (3)–(6) lead to[17,29,30]

$$\nabla^{*2} \phi_e = -\frac{(ka)^2}{(1+\alpha)} [\exp(-\phi_e^*) - \exp(\alpha \phi_e^*)], \tag{8}$$

$$\nabla^{*2}\delta\phi^* - \frac{(\kappa a)^2}{(1+\alpha)}[\exp(-\phi_e^*) + \alpha\exp(\alpha\phi_e^*)]\delta\phi^*,$$

$$= \frac{(\kappa a)^2}{(1+\alpha)}[\exp(-\phi_e^*)g_1^* + \alpha\exp(\alpha\phi_e^*)g_2^*], \quad (9)$$

$$\nabla^{*2}g_1^* = \nabla^*\phi_e^*\nabla^*g_1^* + \gamma Pe_1\mathbf{v}^*\cdot\nabla^*\phi_e^*, \quad (10)$$

$$\nabla^{*2}g_2^* = \alpha\nabla^*\phi_e^*\nabla^*g_1^* + \gamma Pe_2\mathbf{v}^*\cdot\nabla^*\phi_e^*, \quad (11)$$

$$-\nabla\delta p + \gamma\nabla^{*2}\mathbf{v}^* + \nabla^{*2}\phi_e^*\nabla^*\delta\phi^* + \nabla^{*2}\delta\phi^*\nabla^*\phi_e^* = 0, \quad (12)$$

$$\nabla^*\cdot\mathbf{v}^* = 0, \quad (13)$$

Here, $\alpha = -z_2/z_1, \nabla^{*2} = a^2\nabla^2$, $\delta p^* = \delta p[\varepsilon(k_BT/z_1e)^2/a^2], \nabla^* = a\nabla$, $\kappa = [\Sigma_{j=1}^2 n_{j0e}(z_je)^2/\varepsilon k_BT]^2$, $Pe_j = \varepsilon(k_BT/z_1e)^2/\mu D_j$, $\mathbf{v}^* = \mathbf{v}/U^0$, $U^0 = \varepsilon\gamma(k_BT/z_1e)^2/a\mu$, $\gamma = \nabla^*n_0^*$, $n^* = n_0/n_{0e}$, $\phi_e^* = \phi_e/(k_BT/z_1e)$, $\delta\phi^* = \delta\phi/(k_BT/z_1e)$, and $g_j^* = g_j/(k_BT/z_1e)$ with U^0, κ, and Pe_j being a reference velocity, the reciprocal Debye length, and the electric Peclet number of ionic species j, respectively.

We assume the following: (i) The electric potential at a point far away from the particle is uninfluenced by its presence. (ii) The surface of the particle is nonconductive, impenetrable to ionic species, and nonslip. (iii) The net ionic flux vanishes at a point far away from the particle. (iv) The ionic concentration reaches the value $(n_{j0e} + z\nabla n_{j0})$ at a point far away from the particle. (v) On the boundary of the computational domain, because the fluid is not influenced by the particle, it is stagnant. (vi) The inner electric field of the particle is negligible, because the dielectric constant of a rigid dielectric material is usually much smaller than that of an aqueous electrolyte solution. In our study, the computational domain is uncharged and sufficiently large and, therefore, there is no extra electro-osmotic flow due to its presence and its boundary effect is negligible. For a simpler mathematical treatment, we assume that the particle is fixed and the liquid phase moves with the corresponding relative velocity. Therefore, the boundary conditions associated with Eqs. (8)–(13) can be expressed as

$$\mathbf{n}\cdot\nabla\phi_e^* = \sigma_p \text{ on the particle surface}, \quad (14)$$

$$\phi_e^* = 0 \text{ on the boundary of the computational domain}, \quad (15)$$

$$\phi_e^* = 0 \text{ as } |z^*| \to \infty, r^* < \left(\frac{1}{\lambda}\right), \quad (16)$$

$$\mathbf{n}\cdot\nabla^*\delta\phi^* = 0 \text{ on the particle surface}, \quad (17)$$

$$\mathbf{n}\cdot\nabla^*\delta\phi^* = 0 \quad \text{on the boundary of the computational domain}, \quad (18)$$

$$\nabla^*\delta\phi^* = -\beta\gamma\mathbf{e_z} \text{ as } |z^*| \to \infty, r^* < \left(\frac{1}{\lambda}\right), \quad (19)$$

$$\mathbf{n}\cdot\nabla^*g_j^* = 0 \text{ on the particle surface}, \quad (20)$$

$$\mathbf{n}\cdot\nabla^*g_j^* = 0 \quad \text{on the boundary of the computational domain}, \quad (21)$$

$$g_1^* = -z^*\gamma - \delta\phi^* \text{ as } |z^*| \to \infty, r^* < \left(\frac{1}{\lambda}\right), \quad (22)$$

$$g_2^* = \frac{1}{\alpha}z^*\gamma - \delta\phi^* \text{ as } |z^*| \to \infty, r^* < \left(\frac{1}{\lambda}\right), \quad (23)$$

$$\mathbf{v}^* = 0 \text{ on the particle surface}, \quad (24)$$

$$\mathbf{v}^* = -U^*\mathbf{e_z} \quad \text{on the boundary of the computational domain}, \quad (25)$$

$$\mathbf{v}^* = -U^*\mathbf{e_z} \text{ as } |z^*| \to \infty, r^* < \left(\frac{1}{\lambda}\right). \quad (26)$$

In these expressions, $\beta = (D_1 - D_2)/(D_1 + \alpha D_2)$ with D_j being the diffusivity of ionic species j; $z^* = z/a$, $r^* = r/a$, $\lambda = c/b$, and $U^* = U/U^0$; $\mathbf{n}$ is the normal vector directed into the liquid phase; $\mathbf{e_z}$ is the unit vector in the z-direction.

For a simpler mathematical treatment and interpretation of the behavior of a particle, the original problem is partitioned into two subproblems:[31] (i) the particle moves with constant velocity U in the absence of ∇n_0, and (ii) ∇n_0 is applied but the particle remains stagnant. Then the diffusiophoretic velocity of the particle can be determined from a balance of the forces acting on it in the z-direction. These include the electric force F_e and the hydrodynamic force F_d.[5,17,29,30] Let F_{ei} and F_{di} be the z-components of F_e and F_d in subproblem i, respectively, $F_{ei}^* = F_{ei}/\varepsilon(k_BT/z_1e)^2a^2$ and $F_{di}^* = F_{di}/\varepsilon(k_BT/z_1e)^2a^2$ be the corresponding scaled forces, and $F_i = F_{ei} + F_{di}$ be the magnitude of the total force acting on the particle in the z-direction in subproblem i. Then $F_1 = \chi_1 U$ and $F_2 = \chi_2\nabla n_0$, where the proportional constants χ_1 and χ_2 are independent of U and ∇n_0, respectively. Because $F_1 + F_2 = 0$ at steady, U can be expressed as

$$U = -\frac{\chi_2}{\chi_1}\nabla n_0. \quad (27)$$

III. RESULTS AND DISCUSSION

The governing equations, Eqs. (8)–(13), are solved numerically subject to the boundary conditions specified in Eqs. (14)–(26) using FLEXPDE,[32] a finite element based commercial software. To test its applicability, this software is applied to solving the diffusiophoresis of an isolated, uniformly charged sphere in an infinite electrolyte solution, and the numerical results obtained are compared with the corresponding numerical of Prieve and Roman.[5] Figure 2(a) shows the variation of the scaled diffusiophoretic mobility of the particle as a function of its scaled surface potential at two levels of β; both the results of Prieve and Roman[5] and the corresponding results based on the present approach are presented. This figure reveals that the performance of the software adopted is satisfactory.

The present theoretical model is also verified by fitting its special case of uniformly charged particle to the experimental

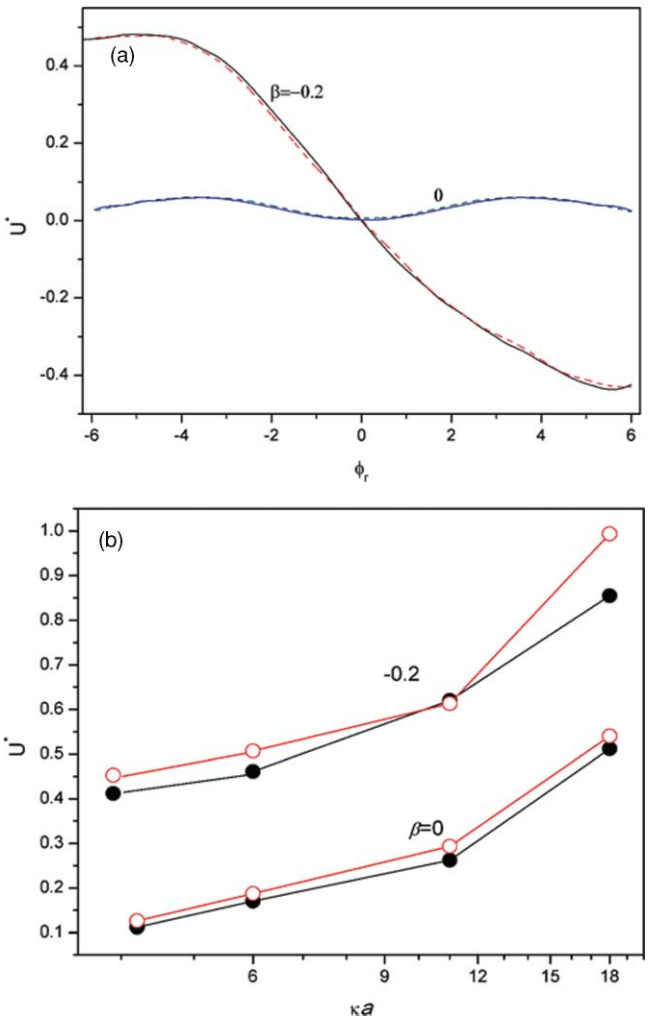

FIG. 2. (a) Variations of the scaled diffusiophoretic velocity U^* as a function of the scaled surface potential ϕ_r for the case of a uniformly charged rigid sphere in an infinite electrolyte solution for two levels of β at $\alpha = 1$, $\kappa a = 1$, and $\sigma_R = \sigma_M = \sigma_L = 4$; solid curve, present study, dashed curve, Prieve and Roman (Ref. 5). (b) Comparison of the experimental data of Ebel *et al.* (Ref. 14), ○, where the diffusiophoresis of a dilute suspension of uniformly charged polystyrene particles in an unbounded aqueous NaCl or KCl solution is conducted with the values predicted by the present theoretical model, ●.

data of Ebel *et al.*,[14] where the diffusiophoresis of a dilute suspension of polystyrene particles in a unbounded aqueous NaCl or KCl solution is conducted. The results obtained are summarized in Fig. 2(b). As seen in this figure, the agreement between the experimental data and the corresponding theoretical results is reasonably well.

In subsequent discussions, the diffusiophoretic behaviors of a particle under various conditions are investigated through numerical simulation. Mesh is refined to assure the convergence of the results obtained throughout the simulation. To examine the effect of electrophoresis arising from the difference in ionic diffusivities, two representative values are chosen for β, namely, $\beta = 0$ and $\beta = -0.2$, which correspond to an aqueous KCl solution ($Pe_1 = Pe_2 = 0.26$) and an aqueous NaCl solution ($Pe_1 = 0.39$ and $Pe_2 = 0.26$), respectively. For illustration, we assume $\alpha = 1$.

A. Dispersion medium with $\beta = 0$

In this case, the effect of electrophoresis is absent. If ∇n_0 is directed to the right, then because the ionic concentration on the right-hand side (RHS) of the particle is higher than that on its LHS, the double layer on the RHS is thinner than that on the LHS.[1,6] Therefore, if the particle is uniformly and positively charged, then the amount of anions (counterions) inside the double layer on the RHS of the particle is greater than that on its LHS, defined as type I DLP by Hsu *et al.*[17] Due to electric attraction, this yields a greater amount of cations (coions) immediately outside the double layer on the RHS of the particle and a greater amount of anions (counterions) on its LHS, defined as type II DLP.[17] Each of these two types of DLP induces an internal electric field with direction opposite to each other. The electric field induced by type I DLP is usually stronger than that induced by type II DLP, and the latter is more significant at a higher surface potential and thinner double layer.

Figure 3 illustrates the influence of the distribution of the surface charge of a particle on the neighboring ionic species in the liquid phase on the plane $\theta = 0$. As seen in Figs. 3(a) and 3(b), the contours of the scaled ionic concentrations for a uniformly charged particle ($R = 1$) are a set of loops enclosing the particle, but not symmetric about $z = 0$ due to the application of ∇n_0. The contours of the scaled net concentration difference, $\delta n^* = [(n_2 - n_{20}) - (n_1 - n_{10})]/n_{e0}$, shown in Fig. 3(c) reveal that the maximum (minimum) of δn^* appears on the RHS (LHS) of the particle, implying that the concentration of anions is higher (lower) on the RHS (LHS), that is, type I DLP is present. The scaled perturbed potential $\delta\phi^*$ shown in Fig. 3(d) has a maximum (minimum) on the LHS (RHS) of the particle, which is consistent with the results illustrated in Fig. 3(c).

As seen in Figs. 3(e) and 3(f), if the particle is nonuniformly charged with $R = -1$, then the contours of the scaled ionic concentrations comprise several set of loops. In this case, more amount of anions are accumulated near both the RHS and the LHS surfaces of the particle where it is positively charged, and more amount of cations are accumulated near the middle surface of the particle, where it is negatively charged, making the contours of δn^* and $\delta\phi^*$ shown in Figs. 3(g) and 3(h) different from those in Figs. 3(c) and 3(d), respectively. Note that both the electric and the hydrodynamic forces acting on the particle are influenced by $\delta\phi^*$, so is its diffusiophoretic velocity.

Figure 4 illustrates the influence of the thickness of double layer, measured by κa, on the scaled diffusiophoretic velocity of a particle U^* at various levels of R ($= \sigma_M/\sigma_R$). As seen in this figure, for the case where the particle is either uniformly charged ($R = 1$) or its middle part is uncharged ($R = 0$) and both its LHS and RHS sides are positively charged, then U^* is positive and decreases with increasing κa. However, if the middle part of the particle is negatively charged and both its right- and left-hand parts are positively charged ($R = -1$), then $U^* < 0$ and $|U^*|$ have a local maximum as κa varies. These behaviors can be explained by the variations of the scaled forces acting on the particle shown in Fig. 5. If the particle is uniformly charged ($R = 1$), then because

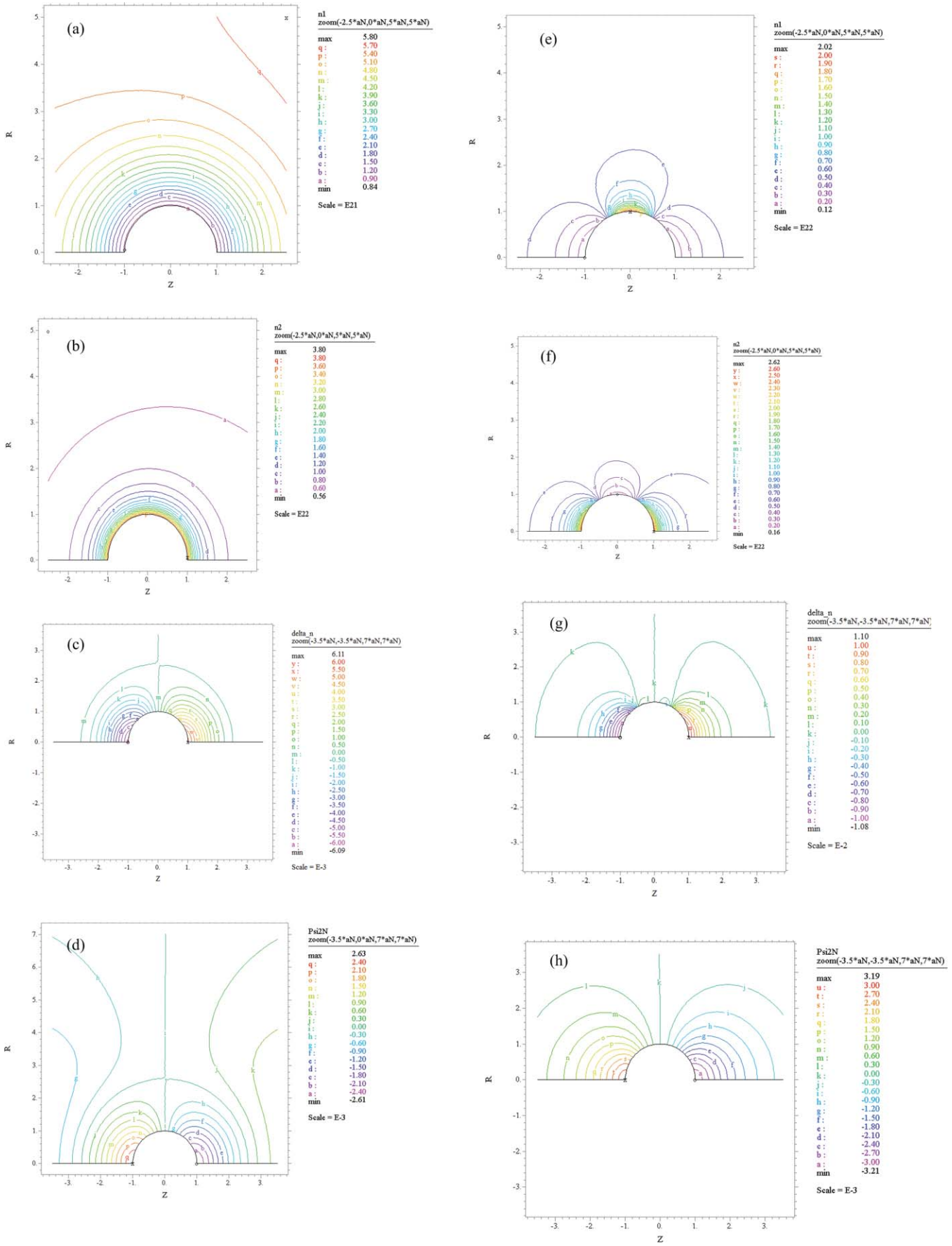

FIG. 3. Contours of the scaled ionic concentrations, the scaled concentration difference $delta\_n(= [(n_2 - n_{20}) - (n_1 - n_{10})]/n_{e0})$, and the scaled disturbed potential $\delta\phi^*$ at $\beta = 0$ and $\kappa a = 1$; (a) and (e), n_1, (b) and (f), n_2, (c) and (g), $delta\_n$, (d) and (h), $\delta\phi^*$; $R = \sigma_M/\sigma_R = 1$ in (a)–(d), $R = -1$ in (e)–(h).

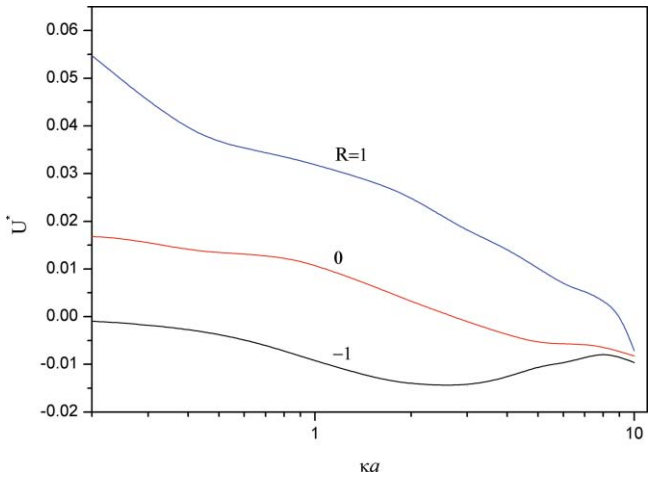

FIG. 4. Variation of the scaled diffusiophoretic velocity U^*as a function of κa for various values of R $(=\sigma_M/\sigma_R)$ at $\beta = 0$, $\kappa a = 1$, $\varphi = 30$, and $\sigma_R = \sigma_L = 4$.

the surface charge density is fixed the corresponding surface potential must decrease with increasing κa. The amount of counterions inside the double layer depends both on its thickness and on the surface potential; the higher the potential and/or the thinner the double layer the greater that amount. However, for a fixed surface charge density, the surface potential and the thickness of double layer vary in opposite directions. As seen in Fig. 5(a), the scaled electric force F^*_{e2} increases with increasing κa, passing through a local maximum, and then decreases with a further increase in κa. The increase in F^*_{e2} at smaller values of κa comes from the increase of the degree of type I DLP with increasing κa, and the decrease in F^*_{e2} at larger values of κa arises from the reduction of the surface potential, and together, they yield a local maximum in F^*_{e2}. Together with the electric force, the hydrodynamic force arising from diffusioosmosis will contribute to the driving force, thereby governing the diffusiophoretic behavior of the particle. The diffusioomosis comprises of an electroosmosis component and a chemiosmosis component. The former comes from the electric field induced by type I and type II DLP and the later from the unbalanced amount of counterions inside the double layer. Note that in the present cases, type I DLP is more significant than type II DLP, and the amount of counterions on the high-concentration side is greater than that on the low-concentration side. Therefore, the hydrodynamic force F_{d2} is negative and tends to drive the particle toward the low-concentration side. The decrease of U^* with increasing κa seen in Fig. 4 at $R = 1$ arises from the decrease in the net scaled force, $(F^*_{e2} + F^*_{d2})$, with increasing κa. If the middle part of the particle is uncharged $(R = 0)$, then the electric force acting on that part of the particle vanishes, and therefore, the total electric force becomes smaller than that for the case where $R = 1$, so is the diffusiophoretic velocity. It is interesting to note in Fig. 5(a) that if the double layer is sufficiently thin (κa sufficiently large), the magnitude of F^*_{d2} can exceed that of F^*_{e2}, yielding a negative U^*, that is, the direction of diffusiophoresis is reversed, as seen in Fig. 4. The variation of F^*_{e2} at $R = -1$ is complicated. For example, if κa is small, then $F^*_{e2}(R = -1) < F^*_{e2}(R = 0)$, but as κa gets large, that trend

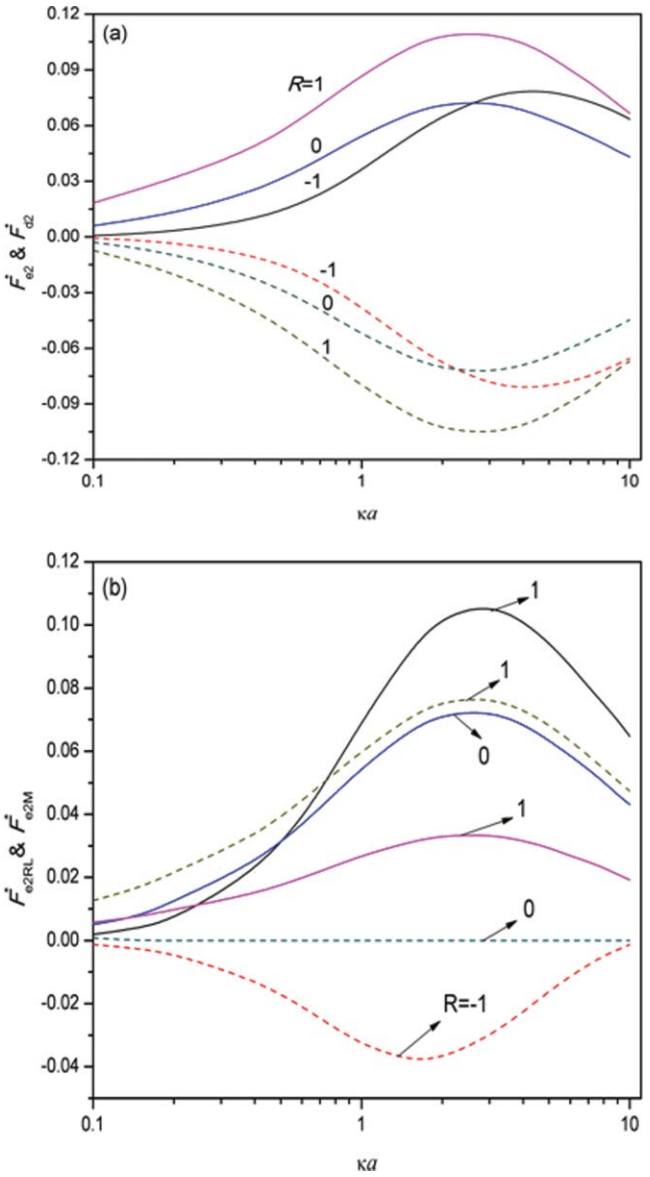

FIG. 5. Variations of the scaled forces F^*_{e2} (solid curves) and F^*_{d2} (dashed curves), (a), and F^*_{e2RL} (solid curves) and F^*_{e2M}(dashed curves), (b), as a function of κa for the case of Fig. 4, where $F^*_{e2RL} = F_{e2RL}/\varepsilon(k_BT/z_1e)^2a^2$ and $F^*_{e2M} = F_{e2M}/\varepsilon(k_BT/z_1e)^2a^2$ are the scaled electric force acting on the right- (left-) hand part of the particle and that on its middle part, respectively.

is reversed. This can be explained by the behaviors of the scaled electric force acting on the middle part of the particle, $F^*_{e2M} = F_{e2M}/\varepsilon(k_BT/z_1e)^2a^2$, and that on its right-hand and left-hand sides, $F^*_{e2RL} = F_{e2RL}/\varepsilon(k_BT/z_1e)^2a^2$, presented in Fig. 5(b). This figure shows that if κa is large, then $F^*_{e2RL}(R = 1) < F^*_{e2RL}(R = 0) < F^*_{e2RL}(R = -1)$, and that trend is reversed if κa is small. If $R = 1$, $F^*_{e2M} > 0$, and if $R = -1$, then $F^*_{e2M} < 0$. In addition, except for the case of $R = 0$, $|F^*_{e2M}|$ increases with increasing κa, passes through a local maximum, and then decreases with a further increases in κa. These behaviors of F^*_{e2M} and F^*_{e2RL} arise from the interaction between the perturbed potentials near the surfaces of the different parts of the particle. Recall that the application of ∇n_0 yields a perturbed potential, type I DLP inside the double layer near the middle particle of the particle, and type II DLP immediately outside that double layer.

At this stage, the types I and II DLP coming from the middle part of a particle alone deserve further discussion. Without losing generality, we assume that the middle part of the particle is negatively charged. As seen in Fig. 6, where we assume that the left- and the right-hand parts of the particle are uncharged, the degrees of types I and II DLP depend upon the thickness of the double layer near the middle surface of the particle. When ∇n_0 is applied, that double layer is polarized and, since the middle part of the particle is negatively charged, the scaled net concentration difference $\delta n^* = [(n_2 - n_{20}) - (n_1 - n_{10})]/n_{e0}$ is negative (positive) on the right- (left-) hand side of the particle, implying that more cations accumulate on its right-hand side [Figs. 6(a)–6(c)], inducing a perturbed potential. In this case, $\delta\phi^* > 0$ on the right-hand side of the particle and $\delta\phi^* < 0$ on its left-hand side [Figs. 6(d)–6(f)], defined previously as type I DLP. Based on the distributions of the scaled net concentration difference $\delta n^*$and the scaled perturbed potential $\delta\phi^*$ shown in Fig. 6, the influence of the DLP of the middle part of a particle on its left- and right-hand parts if they were charged can be summarized as following: (i) If κa is small [Figs. 6(a) and 6(d)], because the double layer is relatively thick, both the left- and the right-hand parts of the particle are influenced only by the type I DLP of its middle part. (ii) If κa takes a medium large value [Figs. 6(b) and 6(e)], because the double layer becomes thinner, both the left- and the right-hand parts of the particle are only slightly influenced by the type I DLP of its middle part, but becomes influenced by the type II DLP of that part. (iii) If κa is large [Figs. 6(c) and 6(f)], then both the left- and the right-hand parts of the particle are influenced only by the type II DLP of its middle part. In this case, the reduction in the surface potential makes the rate of decrease in the degree of type II DLP faster than that of type I DLP.

Let us elaborate further the results shown in Fig. 5 based on the idea that the right- and left-hand parts of a particle can be influenced by the types I and II DLP of its middle part. If both the right- and the left-hand parts of a particle are positively charged, then a negative (positive) perturbed potential is induced on its right- (left-) hand part. Therefore, if the middle part of the particle is positively charged, then the direction of the electric field induced by the type II DLP of that part of the particle is opposite to the electric field induced by the type I DLP on both the right- and the left-hand parts of the particle, thereby reducing the electric force acting on those parts of the particle. On the other hand, if the middle part of the particle is negatively charged, that electric force is raised. Note that if the middle part of the particle is positively (negatively) charged and its right- and left-hand parts are positively charged, the direction of the electric field induced by the type I DLP of the middle part of the particle is similar (opposite) to that induced by the type I DLP of its left- and right-hand parts. Therefore, for example, the result that $F^*_{e2RL}(R = 1) < F^*_{e2RL}(R = 0) < F^*_{e2RL}(R = -1)$ at a sufficiently large κa comes from the influence of the type II DLP of the middle part of the particle on the type I DLP of its right- and left-hand parts, and the result that $F^*_{e2RL}(R = 1) > F^*_{e2RL}(R = 0) > F^*_{e2RL}(R = -1)$ at a sufficiently small κa comes from the effect of the type I DLP of the middle part of the particle. Because ∇n_0 is in the z-direction, the polarization of double layer near the poles of the particle is more serious than that near its middle surface. This implies that the electric force acting on the middle part of the particle comes mainly from the perturbed potential of its right- and left-hand parts. Note that in the present case, the type I DLP of the right-hand and the left-hand parts of the particle, which acts like the type II (I) DLP of its middle part if it is negatively (positively) charged, is more serious than the type I DLP of its middle part. Therefore, if the middle part of a particle is positively (negatively) charged, then it experiences a positive (negative) electric force. As seen in Fig. 5(b), except for the case of $R = 0$, $|Fe^*_{2M}|$ has a local maximum as κa varies. This can be explained by the variation of the degree of the type I DLP of the right- and the left-hand parts of the particle with κa. If κa is not large, that degree increases with increasing κa, so is $|Fe^*_{2M}|$. However, if κa is sufficiently large, then that degree becomes decrease with increasing κa due to the reduction of the surface potential of the particle, so is $|Fe^*_{2M}|$. Based on the variations of the electric force acting on the middle part of the particle discussed previously, in Fig. 4, U^* becomes negative if the middle part of the particle is negatively charged is the result of the decreasing the total electric force acting on the particle due to the negative electric force coming from that part of the particle. The behavior of U^* and the presence of the local maximum in $|U^*|$ as κa vary seen in Fig. 4 can also be explained by the behaviors of F^*_{e2M} shown in Fig. 5(b).

Figure 7 illustrates the influence of R on the scaled diffusiophoretic velocity of a particle U^* at various combinations of φ and κa. Note that the surface areas of the right-hand, the middle, and the left-hand parts of the particle are $2\pi(1 - \cos\varphi_R)$, $2\pi(\cos\varphi_L + \cos\varphi_R)$, and $2\pi(1 - \cos\varphi_L)$, respectively. As seen in Fig. 7, if $R > 1$, then $U^*(\varphi = 60) > U^*(\varphi = 45) > U^*(\varphi = 30)$, and if R is small but positive, then $U^*(\varphi = 60) < U^*(\varphi = 45) < U^*(\varphi = 30)$. These can be explained by the variation of the electric force acting on the middle part of the particle as R and φ increase. The increase in both the fraction and the charge density of the middle part of the particle makes the type I DLP near that part more important and, after combining with the type I DLP of the left- and the right-hand parts of the particle, yields a positive electric force acting on that part of the particle. Since the larger the φ the more significant is the type I DLP of the middle part of the particle, the greater is that electric force. In addition, the larger the R the higher the surface charge density on the middle part of the particle, the greater the electric force acting on the particle, and therefore, the larger the U^*. However, the increase in the surface charge density of the middle part of the particle also raises the degree of the corresponding type II DLP. This has the effect of reducing the degree of the type I DLP of the right- and the left-hand parts of the particle, and therefore, the corresponding electric force decreases, so does U^*. Note that, as pointed out in the discussion of Fig. 6, the influence of the type II DLP of the middle part of a particle on the type I DLP of its right- and left-hand parts is unimportant if κa is either sufficiently small or sufficiently large. This is why in Fig. 7(b), where κa takes a medium large value and the influence of the type II DLP of the middle part of the particle on its rest two parts is significant,

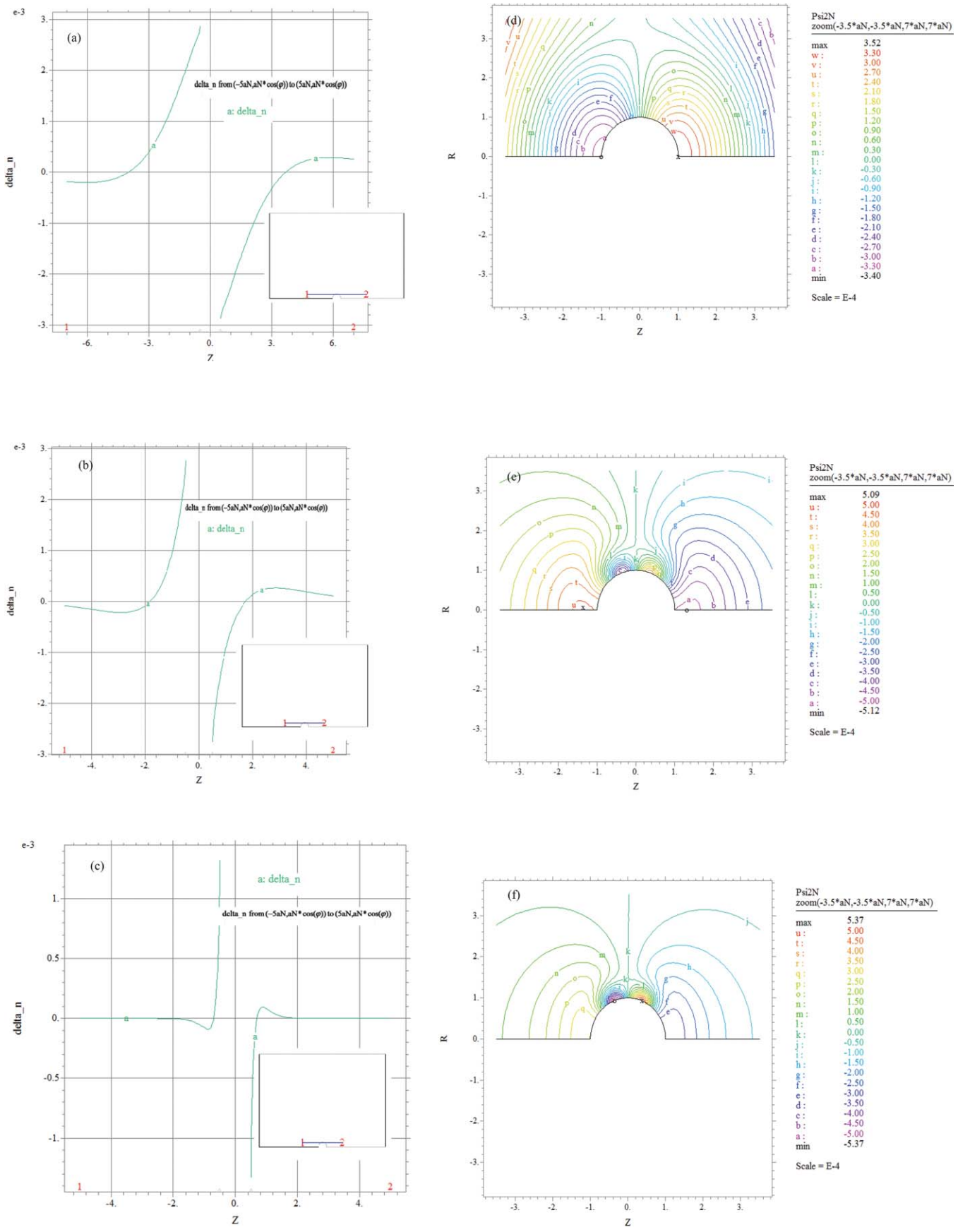

FIG. 6. Spatial variation in the scaled net concentration difference $\delta n^* = [(n_2 - n_{20}) - (n_1 - n_{10})]/n_{e0}$, (a)–(c), and the contours of the corresponding scaled disturbed potential $\delta\phi^*$, (d)–(f), for various levels of κa on the plane $\theta = 0$ at $\beta = 0$, $\sigma_R = \sigma_L = 0$, $\sigma_M = -4$, and $\varphi = 30$. (a) and (d) $\kappa a = 0.5$, (b) and (e) $\kappa a = 3$, (c) and (f) $\kappa a = 5$.

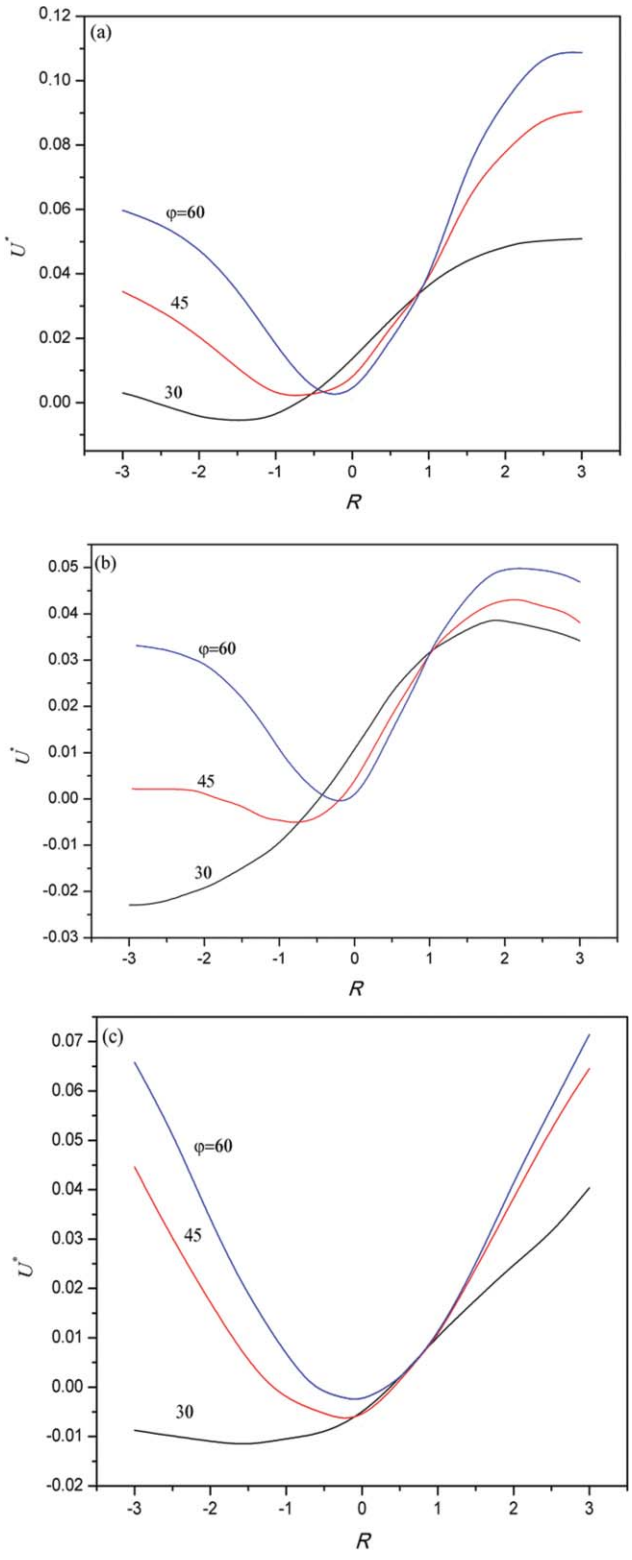

FIG. 7. Variations of the scaled diffusiophoretic velocity U^* as a function of R for various combinations of φ and κa at $\beta = 0$, $\sigma_R = \sigma_L = 4$, and $\sigma_M = 4\sigma_R$. (a) $\kappa a = 0.5$, (b) $\kappa a = 1$, and (c) $\kappa a = 5$.

the decrease of U^* at a sufficiently large R is appreciable, and that decrease is inappreciable both in Fig. 7(a), where κa is small, and in Fig. 7(c), where κa is large. For the same reason, the result of $U^*(\varphi = 60) < U^*(\varphi = 45) < U^*(\varphi = 30)$ at a small positive R can be explained by that if R is small, so is

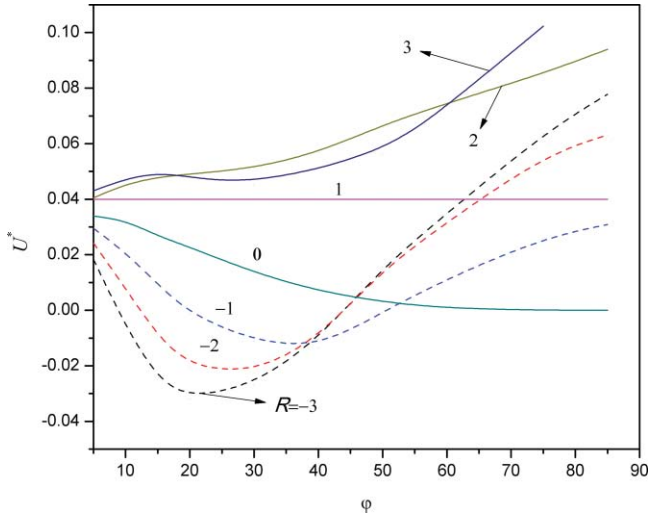

FIG. 8. Variations of the scaled diffusiophoretic velocity U^* as a function of φ at various values of R at $\beta = 0$, $\sigma_R = \sigma_L = 4$, $\sigma_M = 4\sigma_R$, and $\kappa a = 1$.

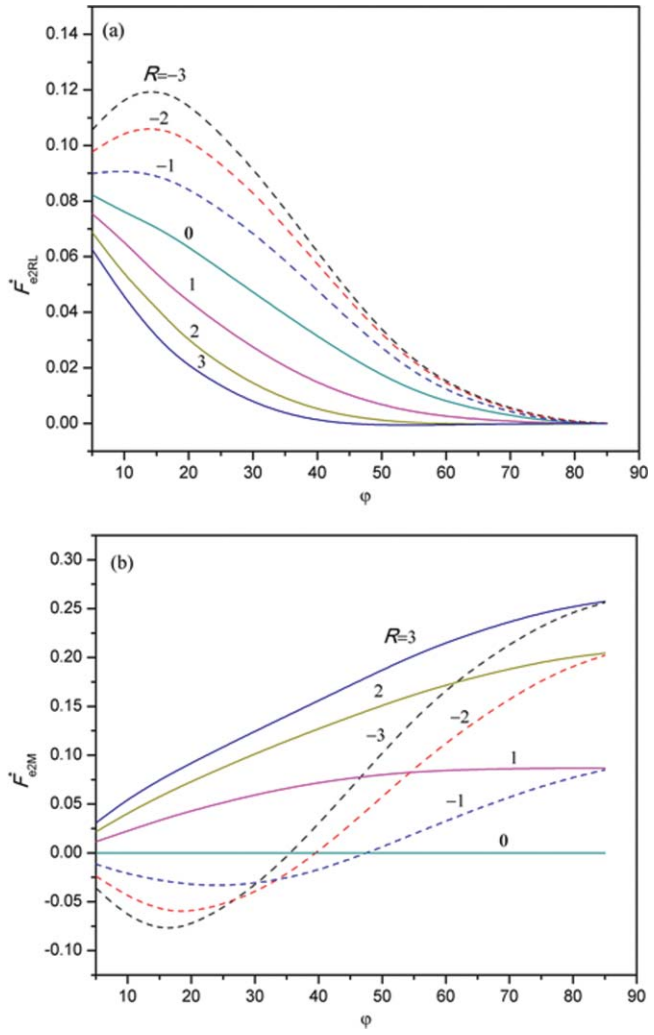

FIG. 9. Variations of the scaled electric force acting on the right- (left-) hand part of the particle F^*_{e2RL} (solid curves) and that on the its middle part F^*_{e2M} (dashed curves) for the cases of Fig. 8.

the electric force acting on the middle part of the particle. If $R < 0$ and $|R|$ are sufficiently large, then except for the case of $\varphi = 30$, $\kappa a = 0.5$ [Fig. 7(a)], the particle is driven toward the low-concentration side ($U^* < 0$) when φ is small and toward the high-concentration side when φ is large. In addition $|U^*|$ decreases with decreasing $|R|$ except for case of $\varphi = 30$ in Fig. 7(c) ($\kappa a = 5$). Again, these can be explained by the behavior of the electric force acting on the middle part of the particle. This force comprises three components: the force coming from the type I DLP of the middle part of the particle, that coming from the corresponding type II DLP, and that coming from the type I DLP of the left- and the right-hand parts of the particle. The first component is positive and the rest two components are negative. If both φ and $|R|$ are large, then the type I DLP of the middle part of the particle is important and the corresponding surface charge density is high, yielding a great positive electric force acting on that part of the particle, and the particle is driven toward the high-concentration side. If φ is small and $|R|$ is large, then because the type I DLP of the middle part of the particle is unimportant, the corresponding type II DLP and the type I DLP of the left- and the right-hand parts of the particle dominate, driving the particle toward the low-concentration side. As seen in Fig. 7, except for the cases of $\varphi = 30$, $R < 0$, and $\kappa a = 0.5$ in Fig. 7(a), and that of $\varphi = 30$, $R < 0$, and $\kappa a = 5$ in Fig. 7(c), $|U^*|$ decreases with decreasing $|R|$. This is because both the degree of the type I DLP and the surface charge density of the middle part of the particle decrease with decreasing $|R|$, so does the contribution to the electric force by that part of the particle. Those exceptions in Figs. 7(a) and 7(c) can be explained as following. In Fig. 7(a) ($\kappa a = 0.5$), if $\varphi = 30$ and $R < 0$, then as $|R|$ decreases, U^* decreases from a positive value to become negative, passes through a negative local minimum, and then becomes positive again; similar behavior is observed in Fig. 7(c) ($\kappa a = 5$) except that U^* is all negative. In Fig. 7(a), κa is small, the electric field induced by the type I DLP of the middle part of the particle also influences its left- and right-hand parts, thereby reducing the influence of the type I DLP of those parts, which acts like the type II DLP of the middle part of the particle. In addition, if $|R|$ is sufficiently large, then the influence of the type I DLP of the middle part of the particle cancels with that of its left- and right-hand parts, thereby raising the positive electric force acting on the middle part of the particle and the total positive electric force acting on the particle, yielding a positive U^*. The observation in Fig. 7(a) ($\kappa a = 0.5$), if $\varphi = 30$ and $R < 0$ that as $|R|$ decreases, U^* decreases from a positive value to become negative, passes through a negative local minimum, and then becomes positive again, arises from the competition between the reduction in the degree of the type I DLP and that in the charge density of the middle part of the particle as $|R|$ decreases. The decrease in the degree of the type I DLP of the middle part of the particle reduces its influence on the type I DLP of its rest two parts, and therefore, the significance of the type I DLP of those parts of the particle, which acts like the type II DLP of its middle part, increases, thereby reducing U^*. As $|R|$ decreases, the decrease in the surface charge density, and therefore, the amount of negative surface charge of the middle part of the particle yields a decrease in the negative electric force acting on that part of the particle, thereby reducing $|U^*|$, and if $|R|$ is sufficiently small, U^* becomes positive. The observation that the behavior of U^* in Fig. 7(c) ($\kappa a = 5$) is similar to that in Fig. 7(a) ($\kappa a = 0.5$) can be explained by the same reasoning. The result that $U^* < 0$ in Fig. 7(c) for the case where $\varphi = 30$ and $R < 0$ arises from that the degree of the type I DLP of the right- and the left-hand parts of the particle is enhanced slightly by the type II DLP of its middle part. In contrast, the degree of the type I DLP of the right- and the left- hand parts of the particle in Fig. 7(a) is reduced by the type I DLP of its middle part.

The variations of U^* as a function of φ at various levels of R are illustrated in Fig. 8, and the corresponding variations in the scaled electric forces acting on various parts of a particle presented in Fig. 9. Note that, regardless of the sign of the surface charge, the type I DLP of the middle part of the particle always induces a positive electric force acting on that part of the particle. In contrast, the electric force induced by the type I DLP of the left- and the right-hand parts of the particle acting on its middle part can be either positive or negative, depending upon the sign of their surface charge. This force is also influenced by the electric force coming from the type II DLP of the middle part of the particle. If φ is small, then $U^* > 0$, regardless of the level of R, and it increases with increasing R. This is because if the fraction of the middle part of the particle is small, then the electric driving force comes mainly from the type I DLP of its right- and left-hand parts. This type I DLP generates a positive force, which is large when φ is small, acting on the right- and the left-hand parts of the particle, yielding a positive U^*. Note that, as shown in Fig. 9, if $R > 0$, then F^*_{e2M} and F^*_{e2RL} have the same sign, and they have different sign if $R < 0$. The result that U^* increases with increasing R arises from that F^*_{e2M} increases with increasing R. As φ increases, the significance of the type I DLP, that of the type II DLP, and the total amount of surface charge of the middle part of the particle all increase. If $R > 0$, the increase of U^* with increasing φ arises from that the type I DLP of the middle part of the particle and that of its rest parts all drive the middle part of the particle, and therefore, the whole particle toward the high-concentration side. On the other hand, if $R < 0$, because the rate of increase in the significance of the type I DLP of the middle part of the particle as φ increases is not fast enough compared with that of the type II DLP of its middle part and that of the type I DLP of its rest parts, F^*_{e2M} and, henceU^* decreases accordingly. In addition, the smaller the $|R|$ the smaller the negative force coming from the type II DLP of the middle part of the particle and that from the type I DLP of its rest two parts acting on its middle part, and therefore, the smaller the $|U^*|$. However, if φ increases further, so is the fraction of the middle part of the particle and the significance of the corresponding type I DLP. This has the effect of reducing $|Fe^*_{2M}|$, and therefore, $|U^*|$, yielding the presence of a local maximum in $|U^*|$. If φ is sufficiently large, the electric force acting on the middle part of the particle becomes positive, driving that part of the particle, and therefore, the whole particle toward the high-concentration side. Figure 8 reveals that the relative magnitudes of U^* for various negative values of R at large values of φ become different

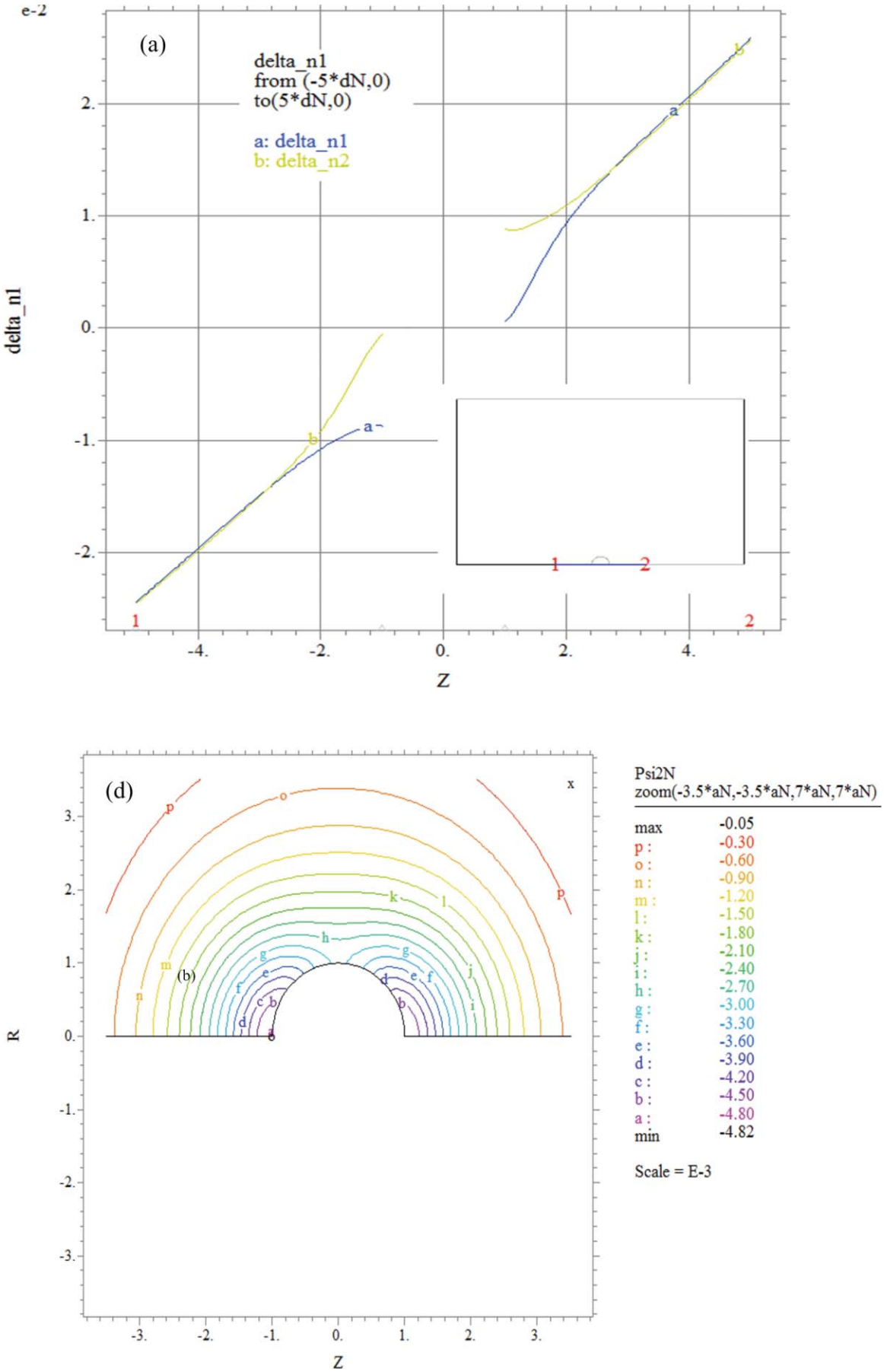

FIG. 10. Spatial variations in the scaled net concentration difference $delta\_n(=[(n_2-n_{20})-(n_1-n_{10})]/n_{e0})$ and the scaled perturbed potential $\delta\phi^*$ on the plane $\theta=0$ at $\beta=0$, $\sigma_R=-\sigma_L=6$, $\varphi=0$, and $\kappa a=1$.

from that at small values of φ. For instance, if φ is large, then $U^*(R = -3) > U^*(R = -2) > U^*(R = -1) > U^*(R = 0)$, but that order is reversed if φ is small. Again, this arises from the behavior of F^*_{e2M} shown in Fig. 9(b). In the present case, because the middle part of the particle is large, the amount of surface charge on that part of the particle is large, and the corresponding type I DLP is important, making F^*_{e2M}, and therefore, the total electric force large. Note that if φ takes a medium large value (e.g., 30), then $U^*(R = 3) < U^*(R = 2)$, but that order is reversed for other values of φ. This arises from the influence of the effect of type II DLP of the middle part the particle on its left- and right-hand parts.

Let us consider next the special case where the particle is divided into the left- and the right-hand halves with its right- (left-) hand half positively (negatively) charged, that is, $\sigma_R = -\sigma_L = \sigma(> 0)$. If ∇n_0 is applied, the double layer on the high-concentration (right-hand) side is compressed and that on the low-concentration (left-hand) side is expanded. This polarization of the double layer can be interpreted by the mechanism suggested by Dukhin and co-workers,[1,6] which is defined as type I DLP by Hsu *et al.*[17] In the present case, because on the right- (left-) hand side of the particle the tangential component of the Stern potential points from the high- (low-) to the low- (high-) concentration side, anions accumulate on the right-hand side of the particle and cations are expelled from the left-hand side. Therefore, as seen in Fig. 10, the scaled perturbed concentration of anions, δn^*_2, is higher than that of cations, δn^*_1, where $\delta n^*_j = \delta n_j / n_{j0e}$, $j = 1,2$, and a negative perturbed potential $\delta\phi^*$ is induced on both sides of the particle. Note that the maximum of $|\delta\phi^*|$ occurs at the poles of the particle ($r = a$, $z = \pm a$), and its value decreases along the surface of the particle to its equator ($r = a$, $z = 0$).

Figure 11 shows the variations of U^* as a function of κa at various values of σ (> 0) for the case where the particle is divided into the left- and the right-hand halves. The former is negatively charged and the latter is positively charged with $\sigma_R = -\sigma_L = \sigma$. Because the signs of the charge on the two halves of the particle are different, the type II DLP of its one half reduces the degree of the type I DLP of its other half, yielding a small electric force. In addition, due to the presence of the circulation flow near the particle surface, as illustrated in Fig. 12, the hydrodynamic drag dominates and, therefore, the total force acting on the particle is negative, so is U^*. The presence of the circulation flows arises from that although some of cations must be expelled from the left-hand side of the particle due to the application of ∇n_0; excess cations are still present in that region since the left-hand half of the particle is negatively charged. These excess cations tend to migrate from the equator of the particle to its left-hand pole, dragging fluid flow in that direction. Similarly, on the right-hand side of the particle, anions tend to migrate from the pole of the particle to its equator. In a study of the effect of the nonuniform surface charge density on the self-electrophoresis of a spherical particle, Qian and Joo[28] proposed that, due to the accumulation of excess counterions, the positive (negative) charged part of a particle acts like the source (sink) of electric field. This implies that there present a local electric field on the right-hand side of the particle directing from the particle surface to the fluid and a local electric field on the left-hand side of the particle directing from the fluid to the particle surface. The superposition of these two local electric fields yields the flow field shown in Fig. 12, where clockwise circulation flows are present on both sides of the particle. These circulation flows contribute significantly to the pressure component of the hydrodynamic drag. In addition, because the left-hand half of the particle is negatively charged, it is difficult for anions to move from the right-hand side of the particle to its left-hand side. Therefore, anions tend to accumulate on the right-hand side of the particle. This also contributes to the pressure component of the hydrodynamic drag, and therefore, raises that force, which drives the particle toward the low-concentration side. Note that for a fixed κa, the higher the surface charge density, the higher the surface potential, the larger the amount of anions (cations) attracted into the double layer on the right- (left-) hand side, and therefore, the greater the hydrodynamic drag acting on the particle, yielding a more negative U^*. If the surface charge density is fixed, then the larger the κa the more the amount of counterions in the double layer, the greater the hydrodynamic force exerting on the particle, and therefore, the larger the $|U^*|$. However, if the surface charge density is fixed, an increase in κa also yields a decrease in the surface potential and, therefore, a decrease in the amount of counterions in the double layer, yielding a decrease in $|U^*|$. The competition of these two effects leads the presence of a local maximum in $|U^*|$ seen in Fig. 11.

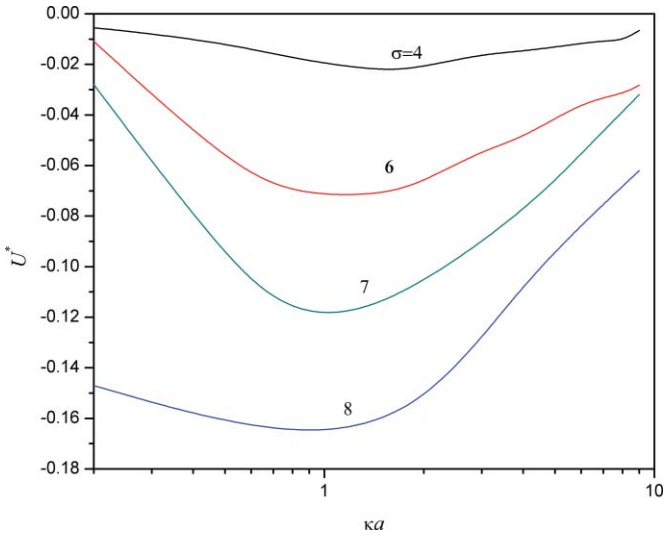

FIG. 11. Variations of the scaled diffusiophoretic velocity U^* as a function of κa for various levels of σ at $\beta = 0$, $\sigma_R = -\sigma_L = \sigma$, and $\varphi = 0$.

If the scaled surface charge density of the right-hand part of the particle, σ_R, is fixed and that on its left-hand part, σ_L, varies, then because both the electric force coming from type I DLP and the flow field near the particle vary, yielding the results shown in Fig. 13. As seen in this figure, if $|S|$ ($S = \sigma_L/\sigma_R$) is large and κa is small, then because the surface charge density on the left-hand half of the particle is high, the corresponding type I DLP is significant, and the hydrodynamic drag acting on the particle is small because the double layer is thick, U^* is positive. As κa gets large, the hydrodynamic drag dominates, and the particle is driven toward the low-concentration side ($U^* < 0$). It is interesting to see in

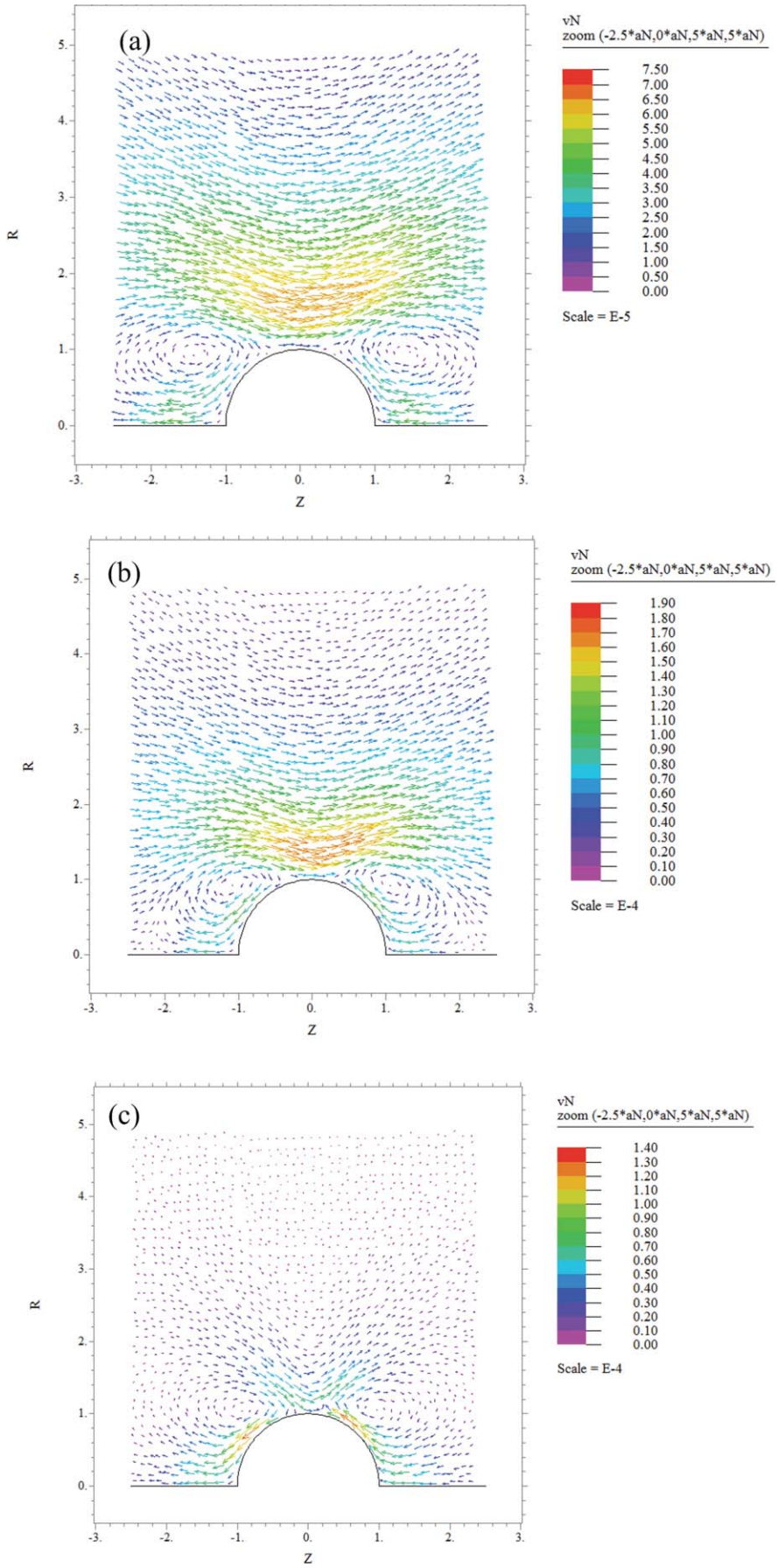

FIG. 12. Contours of the scaled fluid velocity in the second subproblem on the plane $\theta = 0$ at $\beta = 0$, $\varphi = 0$, $\kappa a = 1$, and $\sigma_R = -\sigma_L = 6$. (a) $\kappa a = 0.5$, (b) $\kappa a = 1$, (c) $\kappa a = 5$.

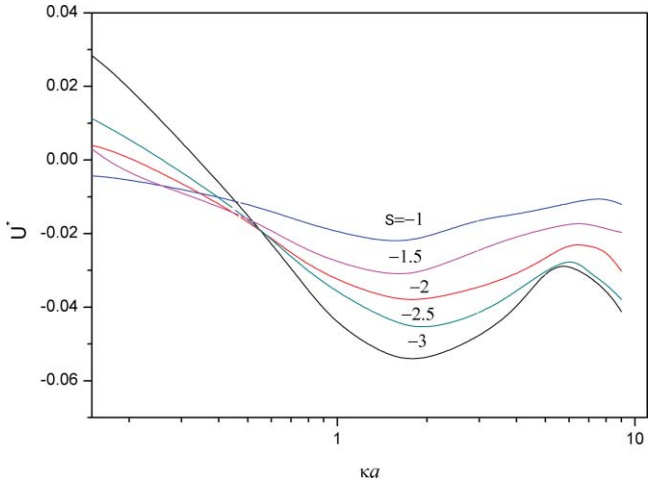

FIG. 13. Variations of the scaled diffusiophoretic velocity U^* as a function of κa at various values of $S\,(=\sigma_L/\sigma_R)$ at $\beta = 0$, $\varphi = 0$, and $\sigma_R = 4$.

this case that U^* has both a local negative minimum and a local negative maximum. The presence of the local minimum in U^* can be explained by the same reasoning as that employed in the discussion of Fig. 11. Note that the larger the $|S|$ the more significant the type I DLP near the left-hand half of the particle, yielding a more positive (negative) U^* at smaller (larger) κa, where the hydrodynamic drag is smaller (greater) due to thicker (thinner) double layer. If κa is sufficiently large, then the decrease in the hydrodynamic drag due to the decrease in the surface potential is compensated by the increase in that drag due to the decrease in the thickness of double layer, and therefore, $|U^*|$ increases, yielding the presence of the local maximum.

B. Dispersion medium with $\beta \neq 0$

If the diffusivity of cations is different from that of anions, then $\beta \neq 0$ and the effect of electrophoresis need be taken in to account.[4,5,17] In this case, as expressed in Eq. (19), a background electric field is induced, the direction of which is opposite to that of ∇n_0. This background electric field drives a positively (negatively) charged particle toward the low-(high-) concentration side. As pointed out by Prieve and Roman[5] and Hsu *et al.*,[29] the electrophoresis effect can have a significant influence on the diffusiophoretic behavior of a particle. As seen in Fig. 14, if this effect is present and the middle part of the particle is positively charged with a charge density higher than its rest parts ($R > 1$), then the larger the R the more the amount of positive charge on the surface of its middle part, the greater the negative electric force coming from the electrophoresis effect and, therefore, it tends to move toward the low-concentration side with $|U^*|(\varphi = 60) > |U^*|(\varphi = 45) > |U^*|(\varphi = 30)$. For $R \leq 1$, $|U^*|$ decreases with decreasing R when $U^* < 0$, and increases with decreasing R when $U^* > 0$. The former is because the amount of surface charge of the middle part of the particle decrease with decreasing R, and therefore, the total amount of surface charge of the particle, which is proportional to the averaged surface charge density $\overline{\sigma}$, decreases accordingly, with $|\overline{\sigma}|(\varphi = 60) < |\overline{\sigma}|(\varphi = 45) < |\overline{\sigma}|(\varphi = 30)$. The later is because

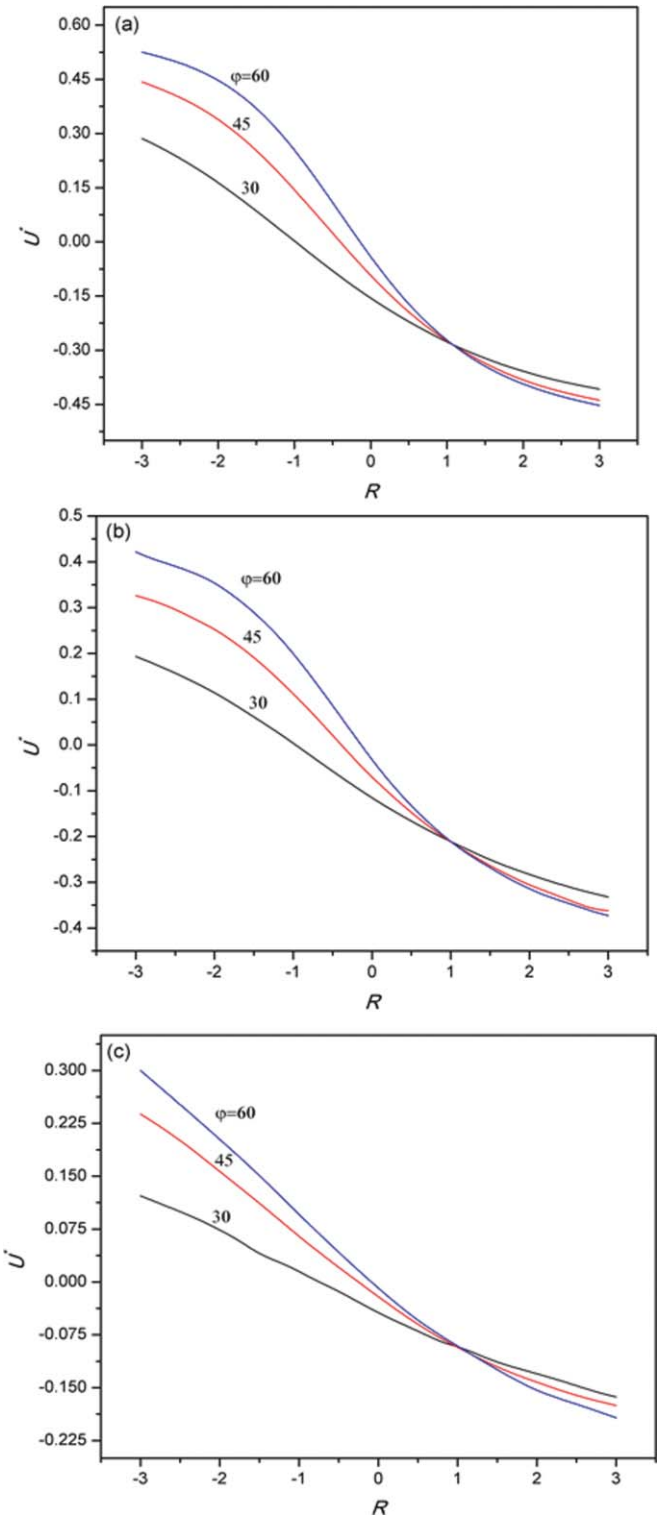

FIG. 14. Variations of the scaled diffusiophoretic velocity U^* as a function of R for various combinations of φ and κa at $\beta = -0.2$, $\sigma_R = \sigma_L = 4$, and $\sigma_M = R\sigma_R$. (a) $\kappa a = 0.5$, (b) $\kappa a = 1$, and (c) $\kappa a = 5$.

both the amount of negative surface charge of the middle part of the particle and that of the particle increase with decreasing R, with $|\overline{\sigma}|(\varphi = 60) > |\overline{\sigma}|(\varphi = 45) > |\overline{\sigma}|(\varphi = 30)$. Figure 14 shows that $|U^*|$ decreases with increasing κa, which is consistent with the observation of Prieve and Roman.[5] This might be caused by that as κa increases, so are the amount and the concentration of ions inside the double

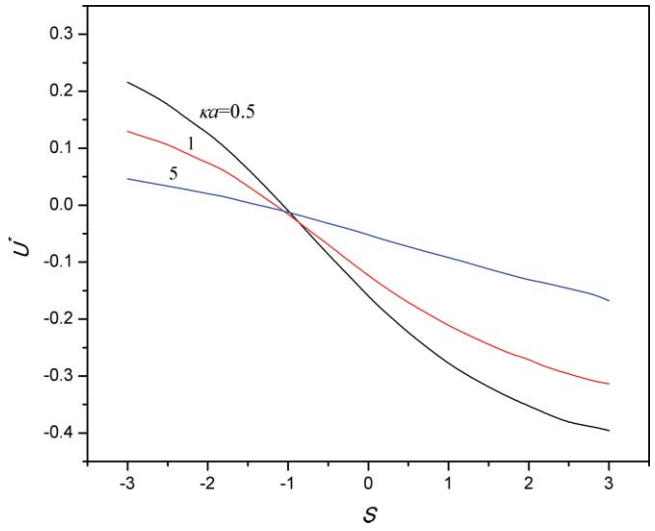

FIG. 15. Variations of the scaled diffusiophoretic velocity U^* as a function of S for various levels of κa at $\beta = -0.2$, $\sigma_R = 4$, $\sigma_L = S\sigma_R$, and $\varphi = 0$.

layer, yielding an increase in the hydrodynamic drag acting on the particle, and therefore, a decrease in $|U^*|$.

Figure 15 illustrates the variations of the scaled diffusiophoretic velocity of a particle U^* as a function of S $(= \sigma_L/\sigma_R)$ at various values of κa for the case where the particle is divided into two equal halves. In this case, the net surface charge density $\overline{\sigma}$ can be reflected by the value of S. For instance, if $S < -1$ $(S > -1)$, then $\overline{\sigma}$ is negative (positive), and the larger the $|S|$ the larger the $\overline{\sigma}$. Figure 15 reveals that if $S < -1$, then $U^* > 0$, and if $S > -1$, then $U^* < 0$. Note that if $S = -1$, then although $\overline{\sigma} = 0$, U^* still takes a small negative value due to the effect of the chemiphoresis. Figure 15 also suggests that the behavior of the particle is dominated by the electrophoresis effect. For example, if $S < -1$, then because $\overline{\sigma} < 0$ and the presence of the electrophoresis effect, U^* is positive, which is different with that in Fig. 13, where $\beta = 0$ and the corresponding velocity U^* is negative. Again, the behavior of U^* depends mainly upon the variations of the surface potential and the hydrodynamic force acting on the particle as κa varies.

IV. CONCLUSIONS

The influence of the nonuniform charged conditions of a spherical particle, where both the level and the sign of the surface charge density of each part of the particle can be different, on its diffusiophoretic behavior in an electrolyte solution is investigated theoretically. In this case, the application of a concentration gradient yields complicated concentration, electric, and flow fields near the particle, leading to profound and interesting diffusiophoretic behaviors. If the electrophoresis effect coming from the difference in the ionic diffusivities is unimportant, we conclude the following: (i) For a fixed surface charge density, the strength of the electric field coming from type I DLP depends upon the amount of countertions inside the double layer, which is related to the surface potential and the thickness of double layer. In this case, because type I DLP dominates, a nonuniformly charged particle always moves toward the high-concentration side. In addition, the lower the surface potential, the less significant the type I DLP, the smaller the electric driving force, and therefore, the smaller the diffusiophoretic velocity of the particle is. (ii) If the particle comprises the right-hand, the middle, and the left-hand parts, with its middle part charged differently, both in sign and in density, with the rest two parts, then each part of the particle is influenced by the polarized double layers of the other parts. Here, the degrees of the types I and II DLP of each part of the particle depend upon its surface charge density, double layer thickness, and its fraction. If the double layer of the middle part of the particle is sufficiently thick, then its type I DLP influences the other two parts of the particle. On the other hand, if that double layer is sufficiently thin, then the right- and the left-hand parts of the particle are influenced mainly by the type II DLP of its middle part. Because the sign of the middle part of the particle is different from that of its other two parts, the type I DLP of the latter acts like the type II DLP of the former, and therefore, reduces the degree of type I DLP of the former. This implies that the diffusiophoretic direction of the particle can be manipulated by the fraction and the charge density of its middle part. (iii) If all the three parts of a particle are positively (or negatively) charged, because the type II DLP of its middle part can dominate at a suitable fraction of that part, an increase in the surface charge density of that part of the particle can lead to a decrease in the diffusiophoretic velocity of the particle. (iv) If the particle is divided into two halves with its right- (left-) hand half positively (negatively) charged, then, due to the migration of the accumulated ions caused by the type I DLP of each half of the particle, circulation flows are present on both sides of the particle, making the pressure component of the hydrodynamic force, which drives the particle toward the low-concentration side, dominates. (v) If the surface charge density of the left-hand half of the particle is higher than that of its right-hand side, then it can be driven to the high-concentration side if the double layer is sufficiently thick. If the electrophoresis effect coming from the difference in the ionic diffusivities is important, then we conclude the following: (vi) The direction of the background electric field induced by the electrophoresis effect is opposite to that of the imposed concentration gradient and, therefore, drives a particle with a positive (negative) averaged surface charge density to the low- (high-) concentration side. (vii) The diffusiophoretic direction of a particle is determined mainly by its averaged surface charge density: if it is positive (negative), then the particle moves toward the low- (high-) concentration side. (viii) If the surface charge density of a particle is fixed, then the hydrodynamic force acting on the particle plays an important role. In this case, the thicker the double layer the smaller the hydrodynamic force and, therefore, the larger the absolute value of the diffusiophoreic velocity.

ACKNOWLEDGMENTS

This work is supported by the National Science Council of the Republic of China.

[1]S. S. Dukhin and B. V. Deryagin, *Surface and Colloid Science* (Wiley, New York, 1974), vol. 7.

[2]J. L. Anderson, M. E. Lowell, and D. C. Prieve, J. Fluid Mech. **117**, 107 (1982).
[3]J. L. Anderson and D. C. Prieve, Sep. Purif. Methods **13**, 67 (1984).
[4]Y. Pawar, Y. E. Solomentsev, and J. L. Anderson, J. Colloid Interface Sci. **155**, 488 (1993).
[5]D. C. Prieve and R. Roman, J. Chem. Soc., Faraday Trans. 2 **83**, 1287 (1987).
[6]S. S. Dukhin, Z. R. Ulberg, G. L. Dvornichenko, and B. V. Deryagin, Bull. Acad. Sci. USSR Div. Chem. Sci. **31**, 1535 (1982).
[7]A. A. Korotkova and N. V. Churaev, Colloid J. USSR **49**, 881 (1987).
[8]A. A. Korotkova and B. V. Deryagin, Colloid J. USSR **53**, 719 (1991).
[9]W. J. Lechnick and J. A. Shaeiwitz, J. Colloid Interface Sci. **102**, 71 (1984).
[10]P. O. Staffeld and J. A. Quinn, J. Colloid Interface Sci. **130**, 88 (1989).
[11]P. O. Staffeld and J. A. Quinn, J. Colloid Interface Sci. **130**, 69 (1989).
[12]Z. R. Ul'berg, N. N. Ivzhenko, G. L. Dvornichenko, R. O. Buadze, and S. A. Koniashvili, Ukr. Khim. Zh. (Russ. Ed.) **58**, 390 (1992).
[13]P. Goldsmith, H. J. Delafield, and L. C. Cox, Q. J. R. Meteorol. Soc. **89**, 43 (1963).
[14]J. P. Ebel, J. L. Anderson, and D. C. Prieve, Langmuir **4**, 396 (1988).
[15]A. A. Korotkova and B. V. Deryagin, Colloid J. Russ. Acad. Sci. **54**, 717 (1992).
[16]A. Meisen, A. J. Bobkowicz, N. E. Cooke, and E. J. Farkas, Can. J. Chem. Eng. **49**, 449 (1971).
[17]J. P. Hsu, W. L. Hsu, and Z. S. Chen, Langmuir **25**, 1772 (2009).
[18]S. Y. Lee, S. E. Yalcin, S. W. Joo, O. Baysal, and S. Qian, J. Phys. Chem. B **114**, 6437 (2010).
[19]S. W. Joo, S. Y. Lee, J. Liu, and S. Qian, ChemPhysChem **11**, 3281 (2010).
[20]S. Lee, S. Yalcin, S. Joo, A. Sharma, O. Baysal, and S. Qian, Microgravity Sci. Technol. **22**, 329 (2010).
[21]S. E. Yalcin, S. Y. Lee, S. W. Joo, O. Baysal, and S. Qian, J. Phys. Chem. B **114**, 4082 (2010).
[22]R. Golestanian, T. B. Liverpool, and A. Ajdari, New J. Phys. **9**, 126 (2007).
[23]R. Golestanian, T. B. Liverpool, and A. Ajdari, Phys. Rev. Lett. **94**, 220801 (2005).
[24]R. G. Winkler and P. Reineker, J. Chem. Phys. **106**, 2841 (1997).
[25]A. W. M. Gibb and L. K. Koopal, J. Colloid Interface Sci. **134**, 122 (1990).
[26]R. J. Hunter, *Foundations of Colloid Science* (Oxford University Press, London, 1989), vol. 1.
[27]S. Z. Qian, S. W. Joo, W. S. Hou, and X. X. Zhao, Langmuir **24**, 5332 (2008).
[28]S. Z. Qian and S. W. Joo, Langmuir **24**, 4778 (2008).
[29]J. P. Hsu, W. L. Hsu, M. H. Ku, Z. S. Chen, and S. Tseng, J. Colloid Interface Sci. **342**, 598 (2010).
[30]J. Lou and E. Lee, J. Phys. Chem. C **112**, 2584 (2008).
[31]R. W. Obrien and L. R. White, J. Chem. Soc., Faraday Trans. **74**, 1607 (1978).
[32]FLEXPDE *version 2.22, PDE Solutions Inc.*, Spokane Valley, WA, 2001.